Where is the Driving Source for HH 168?

Joel D. Green (University of Rochester), David A. Neufeld (Johns Hopkins University), Dan M. Watson (University of Rochester)

Jets and shocks are observed associated with young stars of all masses, during their earliest phases of development. While the launching mechanisms are not well understood (it is unclear whether the launching point is inside the disk or closer to the pole of the central protostar), protostars need to launch such jets to rid themselves of excess angular momentum that would otherwise cause the system to fly apart.

Herbig Haro objects are small optical emission nebulae that signify the interaction between both broad and collimated flows from young stellar objects and the ambient molecular cloud material. GGD37 is suspected to be an amalgamation of at least two superposed flows (including HH 168) traveling in different directions on the sky. Weaker shocks (less than ~ 10000 K) excite the molecular hydrogen into pure rotational states detectable at IRS wavelengths, while strong shocks completely destroy the molecules and illuminate the ions, in particular several transitions of [Fe II]. The Infrared Spectrograph on board *Spitzer* has enabled us to gather spatial information on a number of higher excitation species, and place greater constraints on the flows, allowing us to separate the chemically. How does the instability of driving sources of Herbig Haro jets affect their surrounding medium, ie. What is the momentum injection rate by the flow into the medium? By studying pre- and post-shock gas, we can determine whether outflows from young stars have greater clumping or dispersive effects on their environment. Do outflows trigger or suppress star formation in the neighborhood? And finally, new observations from the IRS open up the question: exactly where is the protostar that is driving HH 168?

Relation of GGD37 to Large Scale CO Outflow

Spectral Mapping with Spitzer-IRS

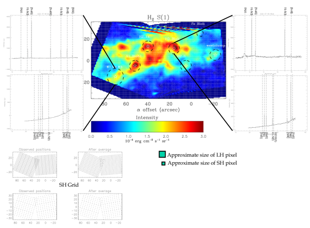

It is possible to create images even with a spectrograph: observing a grid of locations on the sky will produce an image at every wavelength: that is, a three-dimensional dataset containing flux information for every position in RA, dec, and at every wavelength in the map. Using this technique it is possible to produce maps for any spectral line or create continuum maps at any appropriate wavelength. This mapping software utilizes our routines for cleaning damaging pixels, but also makes use of the dense coverage within our maps; different pixels are used to observe the same point on the sky, and thus we can replace bad pixels with good pixels from the same position on the sky. Because of this we can map even faint detections in our spectra.

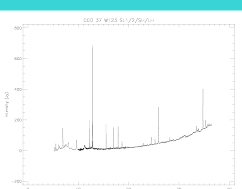

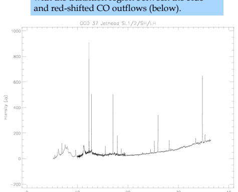

Spectra from the two most energetic regions of the map: the region near the radio source W2 (above), and a region just at the edge of the fine structure emission, but well inside the molecular hydrogen flow, roughly coinciding with the transition region between the blue- and red-shifted CO outflows (below).

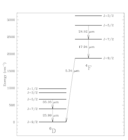

Grotrian diagram of detected [FeII] transitions (figure from Neufeld et al. 2006)

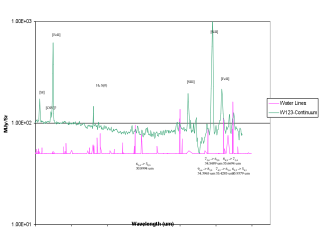

In previous observations of HH54 we were only able to establish upper bounds on the H_2O and OH abundance, but the W1-W2-W3 region of the GGD37 spectra exhibit numerous species of water. We have unprecedented ability to characterize this aspect of the shock using the HITRAN database of molecular lines.

Shown (left) is the spectrum near W2 after subtracting a polynomial continuum, and a comparison of water lines from the HITRAN database. All of the water lines shown appear (more strongly and with many additional lines) in the Class 0 NGC 1333-IRAS 4B (Watson et al. 2007), which exhibits an accretion shock.

GGD 37 in Context

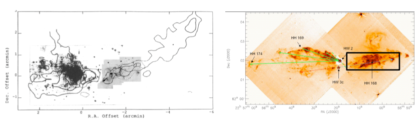

GGD 37 is a collection of Herbig-Haro objects also referred to a Cep A West. Cep A East (shown on the left end of the figure) contains an embedded IR and radio source in its own core. The relationship between Cep A East and West is clearest in CO (blue and red contours, representing blue and red-shifted emission). The location where the red and blue-shifted CO emission switches, in the middle of GGD 37, is also an interesting region in the mid-IR.

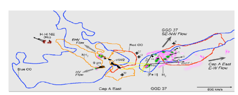

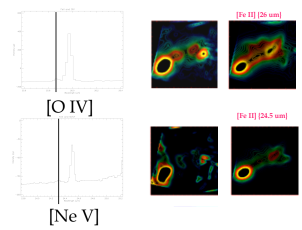

GGD37 brings several new chemical species into the mix. Neufeld et al. (2006) did not detect higher excitation lines such as [Ne III], but the outflow in GGD37 appears to be more energetic. Even more energetic lines such as [OIV] and possibly [NeV] appear in the spectra (left); normally these excitation lines are restricted to photo-ionization regions such as AGN and supernova remnants.

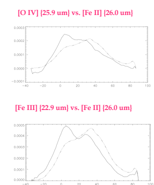

Wavelengths and excitation energies for lines detected in GGD 37 (right). Notably absent is [SIV] 10.5 um, which has an excitation energy of 35 eV and would appear in both SH and SL1 observations.

Line	Module	Wave (um)	Excitation Energy (eV)
Molecular vibrational			
H2_S(0)	LH	28.234407	
H2_S(1)	SH	17.041817	
H2_S(2)	SH	12.285326	
H2_S(2)	SL1	12.324328	
H2_S(3)	SL1	9.7084728	
H2_S(4)	SL1	8.0704654	
H2_S(5)	SL2	6.9395546	
H2_S(6)	SL2	6.1132168	
H2_S(7)	SL2	5.5223064	
HD_R(3)	LH	28.5	
HD_R(4)	LH	23.034	
Fine Structure			
FeII_353	LH	35.35	8
FeII_26	LH	25.969899	8
FeII_245	LH	24.52	8
FeII_18	SH	17.92527	8
FeII_53	SL2	5.3	8
FeIII_229	LH	22.925	16
NeII	SH	12.814849	22
NeII	SL1	12.836706	22
NeIII	SH	15.55	41
SI	LH	25.237379	
SIII	LH	33.48	23
SIII	SH	18.71	23
SiII	LH	34.804445	8
OIV	LH	25.89	55
NeV	LH	24.3	97

Raines (2000) had already noted that the peak of the [Fe II] [1.644 um] emission was significantly shifted to the west of the peak of the molecular hydrogen emission. We find a similar result for all five mid-IR [Fe II] lines relative to all eight mid-IR H_2 lines, but additionally note that the higher ionization lines are even further behind the shock front (left), indicating that we are resolving the cooling region.

Spectral Diagnostics for Momentum Injection Rate

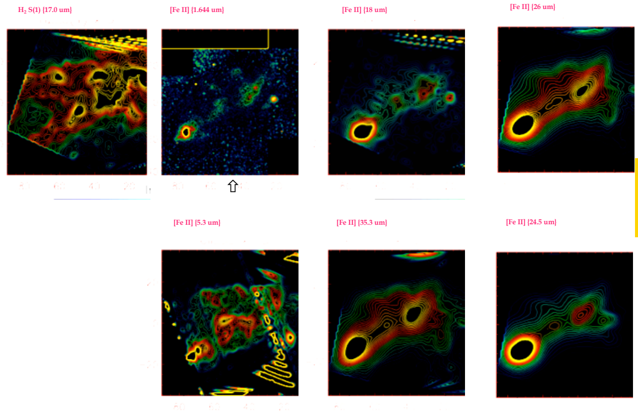

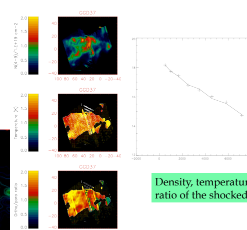

log10(J=2)	18.858046
log10(J=3)	19.058227
log10(J=4)	18.392268
log10(J=5)	18.311546
log10(J=6)	17.575493
log10(J=7)	17.673502
log10(J=8)	16.866391
log10(J=9)	16.488963
T(warm)/K	**433.71849**
log10(N(warm))	19.526577
OPR(warm)	3.2342675
T(hot)/K	**1038.0873**
log10(N(hot))	19.255111
OPR(hot)	1.9809716
log10(N(total)	19.712748
log10(N(4-9)	18.737885
T42	705.76059
T53	685.64383
T64	797.39928
T75	1170.3297
T86	1239.0437
T97	880.83685

Density, temperature, ortho-to-para ratio of the shocked gas

H_2 emission indicates the passage of a weaker shock. Molecular hydrogen survives a C-shock but is dissociated by a J-type shock. Shock excitation of H_2 in this case may indicate a magnetic or radiative precursor to a more powerful (J) J-type shock. The molecular emission peaks generally to the west of the ionic lines; the precursor lights up the cloud ahead of the jet and dissociates the molecules only upon contact with the full force of the J-type shock. Note that the hydrogen is almost evacuated where the dissociative shock has passed.

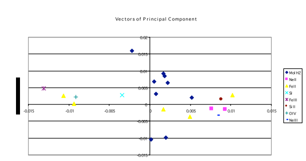

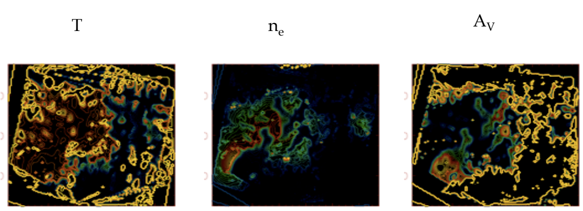

Using a principal component analysis fit to the maps of each spectral line, we determined the principal axis of flow in each case. The results are plotted (right). The clear trend confirms our suspicions that the fine structure emission is predominantly flowing in a different direction than the (lower excitation) molecular hydrogen emission. The SE-NW flow is clearly more energetic than the W-E flow, indicating they may originate from different sources.

The region of GGD 37 containing the most energetic emission surrounds a trio of radio sources in the SE corner. They have been observed in [FeII] 1.644 um by Raines (2000) to display proper motion velocities of ~ 850 km/s (see above).

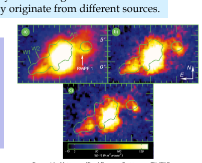

FIGURE 4.8.—MOTION OF [FE II] EMISSION FEATURES IN W1–W3 REGION